

Adaptive Silicon Monochromators for High-Power Insertion Devices. Tests at CHESS, ESRF and HASYLAB

J. P. Quintana,^a M. Hart,^b D. Bilderback,^{c,d} C. Henderson,^c D. Richter,^c T. Setterston,^c J. White,^c D. Hausermann,^e M. Krumrey^e and H. Schulte-Schrepping^f

^aDND-CAT Synchrotron Research Center, APS/ANL Sector 5, Building 400, 9700 Cass Avenue, Argonne, Illinois 60439, USA, ^bDepartment of Physics, Schuster Laboratory, The University, Manchester M13 9PL, UK, ^cCornell High Energy Synchrotron Source, CHESS, Cornell University, Ithaca, New York 14853-8001, USA, ^dSchool of Applied Physics, Cornell University, Ithaca, New York 14853–8001, USA, ^eEuropean Synchrotron Radiation Facility, ESRF, BP 220, F-38043 Grenoble CEDEX, France, and ^fHamburger Synchrotronstrahlungslabor HASYLAB at Deutsches-Elektronen-Synchrotron DESY, Notkestrasse 85, D-22607 Hamburg, Germany

(Received 27 June 1994; accepted 16 August 1994)

X-ray wigglers which produce tens of kilowatts of photon power within the white beam will soon become available at third-generation sources of synchrotron radiation. Insertion devices that produce several kilowatts already exist and we have used those at CHESS, ESRF and HASYLAB to test adaptive 111 silicon water-jet-cooled monochromators at up to 2 kW total incident beam power. This development from earlier work at the Brookhaven National Synchrotron Light Source (NSLS) uses the pressure in the water coolant to provide active compensation of the strain field in the thermal footprint, nulling its effect to within residual variations in Bragg angle of only a few arc seconds. The design is robust, vacuum compatible and uses no moving mechanical parts.

Keywords: high-heat-load optics; crystal monochromators; adaptive optics.

1. Introduction

The concept of jet-cooled monochromators for high-heat-load synchrotron radiation sources was first proposed at a Workshop on High-Heat-Load X-ray Optics held at Argonne National Laboratory in 1989 (Hart, 1989). A particular feature of the design is that the diffracting crystal takes a simple form, which may be just a parallel-sided wafer, leaving free a number of design parameters which permit the correction of the thermal strain field by force transducers such as piezo-electric elements or coolant fluid pressure. In parallel with computer modelling by finite-element analysis (ANSYS) we have tested the performance of the monochromator shown in Fig. 1 on several insertion devices including a wiggler at the Cornell High Energy Synchrotron Source (CHESS), an undulator at the Hamburger Synchrotronstrahlungslabor (HASYLAB) and a multipole wiggler at the European Synchrotron Radiation Facility (ESRF) in Grenoble. In another paper details of the finite-element modelling and double-crystal tests using a laboratory X-ray source are described (Quintana & Hart, 1994).

2. Monochromator design principles

The monochromator wafer is the top surface of the 80 × 22 × 30 mm high silicon-crystal box shown in Fig. 1.

The crystal thickness t is an important parameter which is chosen as a result of the finite-element analysis. The wafer is cooled by a row of jets J whose layout is matched to the shape of the beam footprint following the well known design principles used in laboratory X-ray tubes for many years. The jets cover a useful beam footprint width of 50 mm in these prototypes but the construction is such that the width of useful beam could be extended, as required, to the maximum crystal size available. Two pairs of grooves, marked H in Fig. 1, serve as elastic hinges which allow predominantly cylindrical deformations of the top surface when appropriate forces are applied. In the original proposal it was noted that forces could be applied with piezo-electric elements or by using the pressure in the coolant itself. The latter is the subject of this paper. A further scheme in which the forces for adaption were applied by a pair of pneumatic bellows was tested at about 300 W total power on a multipole wiggler, beamline X-25, at the National Synchrotron Light Source (NSLS) at Brookhaven National Laboratory (Berman & Hart, 1991*a,b*, 1992). That 27-pole hybrid wiggler produces up to 1.8 kW of power from the 2.5 GeV NSLS with a characteristic energy of 4.6 keV (Decker, Galayda, Soloman & Kitamura, 1989).

In response to the thermal footprint of the synchrotron radiation the predominant deformation of the top wafer surface is to become cylindrically bent (Hart, 1990). Coolant pressure inside the silicon-crystal box results in the lower

pair of hinges bending outwards and the upper pair of hinges bending inwards; the top surface becomes concave inwards so as to compensate the convex thermal deformation. This is confirmed by finite-element modelling. An additional function of the tall box sides and the two pairs of hinges is to provide isolation of the base mounting strain from the top diffracting surface. Under the pressure of the coolant it is clear that a very thin wafer would become convex. To avoid that possibility the crystal wafer must not be too thin.

The reason for pursuing the present method is its relative simplicity and inherent vacuum compatibility.

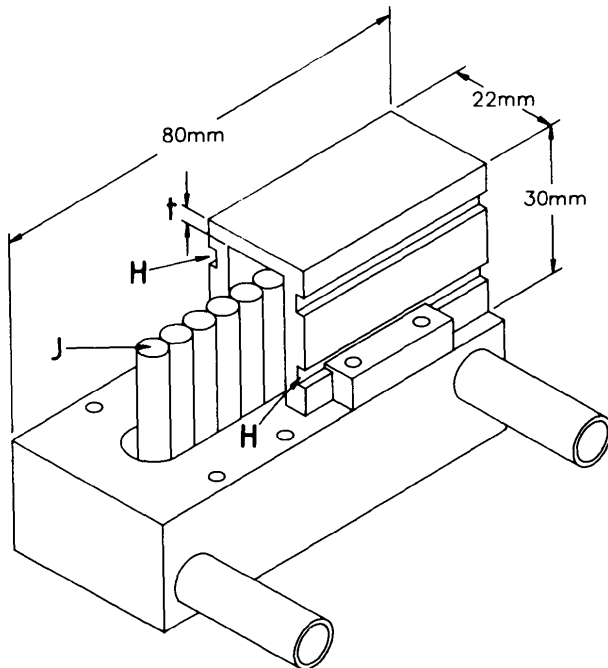


Figure 1
Design of the adaptive silicon-box monochromators. The crystal wafer thickness t is adjustable to suit the anticipated heat load and required adaptive coolant pressure.

3. Tests with the CHESSE wiggler

In 1991 an opportunity arose to use the CHESSE F2 station at 26 m on the 25-pole, permanent-magnet hybrid 1.2 T wiggler beamline (Bilderback *et al.*, 1991). The characteristic energy of this insertion device is 24 keV when the accelerator CESR is running at 5.43 GeV (Finkelstein, 1992). Although this wiggler can produce up to 5 kW of total power at a power density of up to 12 W mm^{-2} , the filtered beam which was then available for these tests contained up to 270 W in the beam footprint on the crystal at a nominal incidence power density of 4.5 W mm^{-2} . In these experiments we were able to demonstrate for the first time the feasibility of the pressure adaptive principle.

The monochromator was set as the first crystal C_1 of a double-crystal diffractometer (Fig. 2) and rocking curves were obtained as a function of water pressure. The 111 diffracted intensity at 12 keV was measured in the ionization chamber I_0 and the 333 Bragg reflection at 33 keV could be simultaneously measured in the second ionization chamber I_D since the aluminium filter was chosen so as to strongly attenuate the fundamental but to transmit the harmonic. The thermal deformation was characterized by measuring the full width at half maximum (FWHM) of the 111 double-crystal rocking curves $I(\theta)$.

At very low beam currents the FWHM of the rocking curve was 7.2 arc sec compared with the theoretical value of 6.4 arc sec. We attribute this small difference to residual mounting strain from the rubber gasket which joins the crystal to the jet-cooling manifold. At 270 W total power and 4.5 W mm^{-2} normal incidence power density the rocking curve FWHM had doubled to 15.0 arc sec. In these experiments we used a 3 mm high slit which has a footprint on the first crystal at 12 keV which is 20 mm wide by 18 mm along the beam.

Tests of the adaption principle were performed with a 1.5 mm high slit with a total power of approximately 100 W at power densities of $3\text{--}4 \text{ W mm}^{-2}$. Fig. 3 shows the 111 rocking curves obtained for the various power loadings listed in the figure caption. The water flow rate was approximately 2 l min^{-1} .

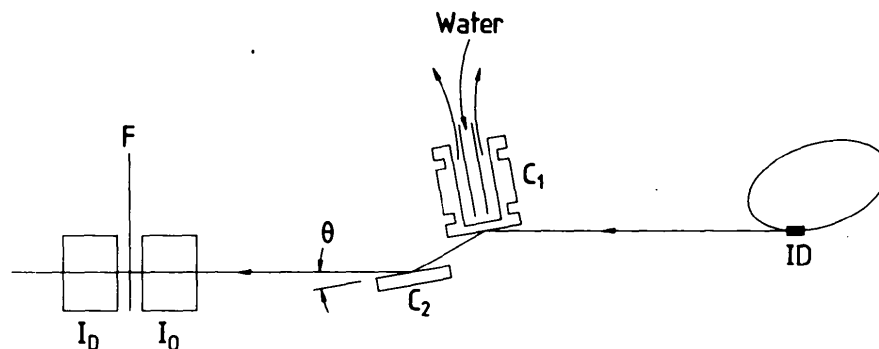


Figure 2
Double-crystal arrangement used to obtain rocking curves $I_0(\theta)$ and $I_D(\theta)$ from the monochromators. Insertion device ID, reference crystal C_2 , F is a low-energy aluminium filter.

As Fig. 3 shows, the FWHM of rocking curve A, which was obtained at the correct compensating water pressure, is only 0.7 arc sec broader than the intrinsic rocking curve of the crystal and 1.5 arc sec wider than the theoretical value for a perfect crystal. Over the footprint area of 9 mm height by 20 mm width the compensation is almost perfect at 100 W total power.

4. Tests with the HASYLAB undulator

By 1993, encouraged by the success of the CHESS results and having completed some of the ANSYS finite-element analysis, we were able to optimize the thickness t of the crystal to suit particular source characteristics. With the dimensions shown in Fig. 1 the optimum thickness of the silicon wafer for compensation pressures of about 2×10^5 kPa and with up to 1 kW total power in the beam footprint is 2.3 mm. A crystal with this dimension was prepared for tests at the HASYLAB undulator.

The BW1 hybrid undulator has been installed on the DORISIII storage ring (Frahm, Weigelt, Meyer & Materlik, 1992, 1994). At 4.5 GeV and 70 mA with a 15.6 mm gap the third harmonic is at 9.1 keV. The filtered beam has 250 W of power in an area 3.3 mm high by 30 mm wide. This is the full width of the undulator beam at the experimental station. Our experiments were performed at 9 keV energy so that the beam footprint on the crystal was 30 mm wide and 15 mm along the beam direction. Whereas the

uncompensated rocking-curve widths, which depend on water pressure as well as X-ray beam power, were around 30 arc sec wide the pressure-compensated width of the 111 curve was only 12.8 arc sec wide (FWHM). A very high degree of compensation was achieved as shown in Fig. 4. The inlet water pressure was 0.8×10^5 kPa and the pressure dropped to half that at the outlet. The mean excess pressure in the crystal was therefore 1.6×10^5 kPa because the monochromator was located inside the vacuum chamber but the water pump was outside at atmospheric pressure. In designing the adaptive crystal box it is important that the absolute pressure drop *across the crystal box* should be taken into account.

Since the 333 theoretical harmonic rocking curve is so narrow we know that the total contribution of thermal and mounting strain is less than 2.5 arc sec. The broadening of the fundamental is almost the same. This indicates that the efficiency of the 111 Bragg reflection from the hot crystal is greater than 80% of theoretical.

5. High-power tests at an ESRF wiggler

Our most recent tests were designed to explore high power loadings using the newly available wiggler on beamline 2 at the ESRF. This 24-pole wiggler has a characteristic energy of 28.8 keV when used in the 6 GeV storage ring and can produce 4.9 kW of radiation at 100 mA current (Kvick & Wulff, 1992; ESRF, 1993). At 6 GeV and 100 mA more than 2 kW of radiation is available in a beam 3 mm high and 50 mm wide in air at the experimental station. Direct measurements of the total power using a 1.5 kg copper calorimeter with no correction for Compton back-scattered

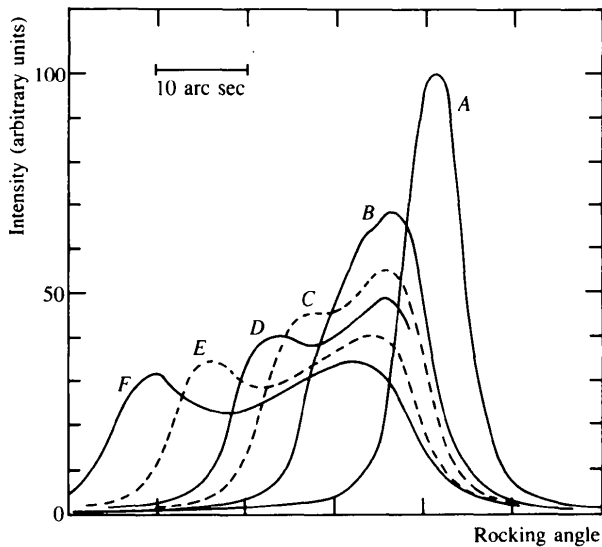


Figure 3
Silicon double-crystal rocking curves obtained at various water pressures. CHESS wiggler, silicon 111 at 12 keV.

Curve	Pressure (10^5 kPa)	Current (mA)	Power (W)	W (mm^2)	FWHM (arc sec)
F	0.71	35.8	118	3.9	35
E	0.79	34.8	115	3.8	29
D	0.87	33.8	112	3.7	23
C	1.00	32.8	108	3.6	19
B	1.07	30.7	101	3.4	14
A	1.26	29.8	98	3.3	7.9

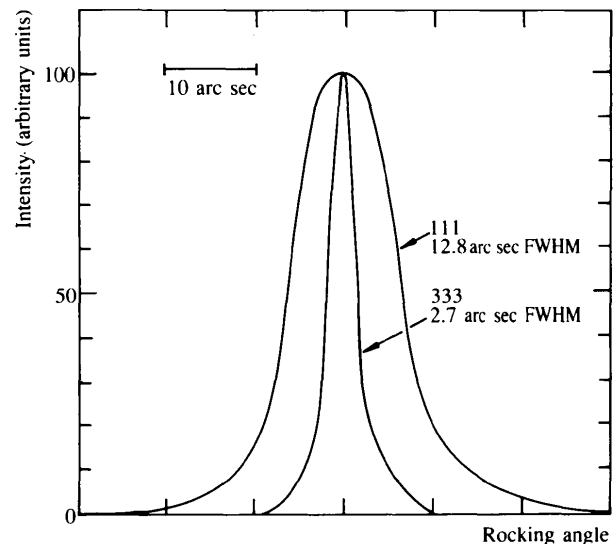


Figure 4
Silicon double-crystal rocking curves obtained at the optimum water pressure. HASYLAB undulator, silicon 111 at 9 keV and 333 at 27 keV.

radiation showed that the available power at 100 mA was at least 1.55 kW. To ensure full illumination of the active area of the monochromator we chose to run at 7 keV which gives a beam footprint 50 mm wide and 10.2 mm along the beam direction on the crystal surface. Water flow rates up to 13 l min^{-1} were obtained at $1.5 \times 10^5 \text{ kPa}$ supply pressure. At 70 mA current (1.4 kW calculated, $> 1.1 \text{ kW}$ measured total power) the best compensated rocking curves were only 7.9 arc sec wide in the 333 harmonic at 21 keV. At these high energies the theoretical rocking curve FWHM is only 1 arc sec so that the measured harmonic width is a good measure of the intrinsic deformation.

Fig. 5 shows some rocking curves obtained at the highest available powers. At the optimum water pressure (curve A) the compensated rocking curve FWHM was 11.0 arc sec at 103 mA while at $1.5 \times 10^5 \text{ kPa}$ (curve B) it was 36.0 arc sec. Clearly, the crystal shape is quite responsive to water pressure changes, but easily controllable. Here the current was 100 mA giving a calculated power of 2.1 kW ($> 1.6 \text{ kW}$ measured).

A variety of effects conspire to make compensation incomplete. The thermal deformation is not just a cylindrical curvature but contains, in addition, a variation of lattice parameter along the beam direction due to the inhomogeneous power density in the synchrotron radiation beam (Hart, 1990). Its power profile in the vertical direction is approximately Gaussian. The X-ray beam is not absorbed in the surface but over a few hundred micrometres depth in the cases described herein so that the deformation field is further complicated. And, of course, the compensating elastic deformation of the crystal box by the water pressure is not a perfect cylinder (Quintana & Hart, 1994).

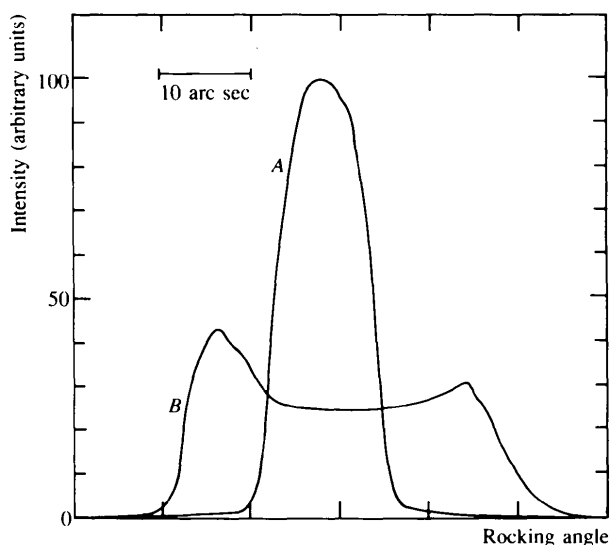


Figure 5
111 Silicon double-crystal rocking curves obtained at two different water pressures. ESRF wiggler at 2 kW total power. A Water pressure optimized at $2.0 \times 10^5 \text{ kPa}$ and B at $1.5 \times 10^5 \text{ kPa}$.

6. Conclusions

The sequence of tests on a variety of synchrotron radiation insertion devices with very different characteristic energies and beam footprints shows that the principle of adaptive optics driven by the coolant pressure alone is viable. If designs are required which work both in vacuum and at ambient atmospheric pressure then the compensation pressure must be greater than 1 atm. In the undulator beam at HASYLAB we worked inside the vacuum chamber so as to maximize the thermal flux. In practice this will be the most likely mode of operation for high-heat-load monochromators. The ultimate requirement is for 'first optical elements', crystals or mirrors, which can cope with the full power and power density of the primary beam.

In some cases these are the best results achieved so far. Reliable extrapolation of these results, through finite-element modelling, should be straightforward up to the current demand limit of about 10 kW. More accurate correction methods might be developed with suitable shaping of the crystal thickness contour, water flow control and additional transducers (Berman & Hart, 1991b).

Besides those insertion devices which we have used in our experiments, several other insertion devices already exist with total powers in the kilowatt range and 10 kW sources are planned. With water flow rates of around 10 l min^{-1} and allowing a coolant temperature rise of 20 K, more than 10 kW of power can be absorbed by this monochromator. The temperature rise in the hot beam footprint is the limiting design parameter (one Darwin width change in Bragg angle is equivalent to a temperature rise of 52 K for the silicon 111 Bragg reflection). The fact that the shape of the compensated crystal is not quite cylindrical is not important at the highest powers (Quintana & Hart, 1994).

By exploring the limits of monochromator thermal design we can also chart areas where adaptive optics might not be essential.

These feasibility experiments were only possible because of the efforts of many facility staff who gave support during the commissioning periods for the various insertion devices which we were able to use. Engineering assistance by Nigel Kelly (Manchester) and Joachim Heuer and Thomas Teichmann (HASYLAB) is especially acknowledged. The research conducted at the Cornell High Energy Synchrotron Source (CHESS), which is supported by the National Science Foundation, was under award No. DMR-9311772. This work is also supported in part by the NSF under grant INT-9008189.

References

- Berman, L. E. & Hart, M. (1991a). *Nucl. Instrum. Methods*, **A300**, 415–421.
- Berman, L. E. & Hart, M. (1991b). *Nucl. Instrum. Methods*, **A302**, 558–562.

- Berman, L. E. & Hart, M. (1992). *Synchrotron Rad. News*, **4**, 22–28.
- Bilderback, D., Henderson, C., Richter, D., Setterston, T., White, J. & Hart, M. (1991). *Fifth High-Heat-Load X-ray Optics Workshop*, 4 February 1991. NSLS, Brookhaven, USA.
- Decker, G., Galayda, J., Soloman, L. & Kitamura, M. (1989). *Rev. Sci. Instrum.* **60**, 1845–1848.
- ESRF (1993). *ESRF Beamline Handbook*, pp. 45–48. ESRF, Grenoble, France.
- Finkelstein, K. D. (1992). *Rev. Sci. Instrum.* **63**, 305–308.
- Frahm, R., Weigelt, J., Meyer, G. & Materlik, G. (1992). *HASYLAB Annu. Rep.* pp. 89–94.
- Frahm, R., Weigelt, J., Meyer, G. & Materlik, G. (1994). *The X-ray Undulator Beamline BW1 at DORISIII*. In preparation.
- Hart, M. (1989). *Workshop on High-Heat-Load X-ray Optics*, ANL/APS/TM-6, pp. 439–459. Argonne National Laboratory, USA.
- Hart, M. (1990). *Nucl. Instrum. Methods*, **A297**, 306–311.
- Kvick, A. & Wulff, M. (1992). *Rev. Sci. Instrum.* **63**, 1073–1076.
- Quintana, J. P. & Hart, M. (1994). In the press.